Competition of long-range interactions and noise at a ramped quench dynamical quantum phase transition: The case of the long-range pairing Kitaev chain

R. Baghran [1], R. Jafari [1,2,3,*] and A. Langari [4,†]

[1]*Department of Physics, Institute for Advanced Studies in Basic Sciences (IASBS), Zanjan 45137-66731, Iran*
[2]*School of Nano Science, Institute for Research in Fundamental Sciences (IPM), Tehran 19395-5531, Iran*
[3]*Department of Physics, University of Gothenburg, SE 412 96 Gothenburg, Sweden*
[4]*Department of Physics, Sharif University of Technology, Tehran 14588-89694, Iran*

(Received 4 April 2024; accepted 16 July 2024; published 2 August 2024)

The nonequilibrium dynamics of long-range pairing Kitaev model with noiseless/noisy linear time dependent chemical potential, is investigated in the framework of dynamical quantum phase transitions (DQPTs). We have shown that for the ramp crossing a single quantum critical point, while the short-range pairing Kitaev model displays a single critical time scale, the long-range pairing induces a region with three DQPTs time scales. We have found that the region with three DQPTs time scales shrinks in the presence of the noise. In addition, we have uncovered that for a quench crossing two critical points, the critical sweep velocity above which the DQPTs disappear enhances by the long-range pairing exponent while decreases in the presence of the noise. On the basis of numerical simulations, we have shown that noise diminishes the long-range pairing inductions.

DOI: 10.1103/PhysRevB.110.064302

I. INTRODUCTION

Long-range interactions have been attracting great interest due to revealing surprising features [1–14]. Long-range systems are often a fascinating approach to analyze the validity of the hypotheses that are otherwise clearly perceived for prototypical short-range systems. The remarkable experimental advancement in ultracold atomic platforms has triggered a plethora of theoretical studies and opened up the possibility of engineering and fine tuning long-range systems with great accuracy [15–20].

Moreover, the unprecedented advancement in recent years is impeccable enough to study the nonequilibrium dynamics of long-range systems in a controlled manner [21–24]. Consequently, over the latest decades, theoretical and experimental research has raised a great deal of interest in nonequilibrium quantum phenomena [25], which has led to the discovery of some intriguing physics, including the observation of Kibble-Zurek phenomena [26,27], discrete time crystals [28], many-body localization [29], and the breaking of ergodicity [30–32].

In recent years, the concept of dynamical quantum phase transitions (DQPTs) have been introduced as nonequilibrium counterparts of thermal phase transitions [33,34]. Within DQPTs real time plays the role of control parameter analogous to temperature in equilibrium phase transitions [35–44]. While the conventional equilibrium phase transition is characterized by nonanalyticities in the thermal free energy, the DQPT is represented by the nonanalytical behavior of dynamical free energy [45–62]. DQPT displays a phase transition between dynamically emerging quantum phases, which takes place during the nonequilibrium coherent quantum time evolution under sudden/ramped quench [63–81] or time-periodic modulation of Hamiltonian [82–89]. Furthermore, analogous to order parameters at equilibrium quantum phase transition, a dynamical topological order parameter is proposed to capture DQPTs [90,91].

DQPT was observed experimentally in several studies [92–98] to confirm theoretical anticipation. Most of the research associated with deterministic quantum evolution generated by ramping or a sudden quench of the Hamiltonian. However, relatively little attention has been devoted to the stochastic driving of thermally isolated systems with noisy Hamiltonian. In any real experiment, the simulation of the desired time-dependent Hamiltonian is imperfect and noisy fluctuations are inevitable [99–102]. Therefore, understanding the effects of noise in such systems is of utmost importance both in designing experiments and comprehend the results [103–107].

Despite numerous studies of DQPTs in a wide variety of long-range quantum systems [108–114], comparatively little attention has been paid to the noise effects [115] on long-range interaction properties. In the present work, we contribute to develop the systematic understanding of the competition between noise and long-range interaction at noisy ramped quench DQPT. For this purpose, we investigate the ramped quench DQPT of long-range pairing Kitaev model [13] in the presence of the white noise with Gaussian distribution [105].

*Contact author: jafari@iasbs.ac.ir; raadmehr.jafari@gmail.com
†Contact author: langari@sharif.edu

We solve an exact master equation for the quench dynamics averaged over the noise distribution. This allows us to study the competition between the near-adiabatic quench dynamics of the gapped modes of the long-range pairing system and the accumulation of noise-induced excitations.

We show that, for the quench across a single critical point, while the long-range pairing induces a region with three DQPTs time scales (three critical modes), this region shrinks in the presence of the noise. In addition, for a quench that crosses two critical points, the critical sweep velocity above which the DQPTs disappear, enhances by the long-range pairing while decreases in the presence of the noise. In other words, the noise has destructive effects on long-range pairing features.

The paper is organized as follows. In Sec. II, the dynamical free energy and dynamical topological order parameter (DTOP) of the two band Hamiltonians are discussed. In Sec. III, we present the model and review its exact solution and equilibrium phase transition. Section IV is dedicated to the numerical simulation of the noiseless case based on the analytical result. The effects of noise on the system is numerically studied in Sec. V. Section VI contains some concluding remarks.

II. QUENCH OF AN INTEGRABLE MODEL AND DYNAMICAL PHASE TRANSITION

A. Dynamical free energy

To study the ramped quench DQPTs, we follow the method used in Refs. [116,117] in the subsequent discussions. Let us consider an integrable model reducible to a two-level Hamiltonian $H_k(\lambda)$ for each momentum mode and the system is initially ($t_i \to -\infty$) prepared in the ground state $|g_k^i\rangle$ of the prequench Hamiltonian $H_k(\lambda_i)$ for each mode. Thereupon the parameter λ is quenched from an initial value λ_i at t_i to the final value λ_f at t_f, following the linear quenching protocol $\lambda(t) = vt$, in such a way that the system crosses the quantum critical point (QCP) at $\lambda = \lambda_c$. Since the adiabatic dynamics breaks in the vicinity of the QCP, the final state $|\psi_k^f\rangle$ (for the kth mode) may not be the ground state of the postquench Hamiltonian $H_k(\lambda_f) = H_k^f$. The postquench state can be written in the form of $|\psi_k^f\rangle = v_k|g_k^f\rangle + u_k|e_k^f\rangle$, ($|u_k|^2 + |v_k|^2 = 1$) where, $|g_k^f\rangle$ and $|e_k^f\rangle$ are the ground and the excited states of the postquench Hamiltonian H_k^f, respectively, with the corresponding energy eigenvalues $\epsilon_{k,1}^f$ and $\epsilon_{k,2}^f$. The nonadiabatic transition probability where the system ends up in the excited state at the end of quench is denoted by $p_k = |u_k|^2 = |\langle e_k^f|g_k^i\rangle|^2$. Therefore, the Loschmidt overlap and the corresponding dynamical free energy [33,34], for the mode k for $t > t_f$ are defined by [116,117]

$$\mathcal{L}_k = \langle\psi_k^f|\exp\left(-iH_k^f t\right)|\psi_k^f\rangle = |v_k|^2\exp\left(-i\epsilon_{k,1}^f t\right) + |u_k|^2\exp\left(-i\epsilon_{k,2}^f t\right), \quad (1)$$

$$g_k(t) = -\frac{1}{N}\log\langle\psi_k^f|\exp\left(-iH_k^f t\right)|\psi_k^f\rangle, \quad (2)$$

respectively, where N is the size of the system.

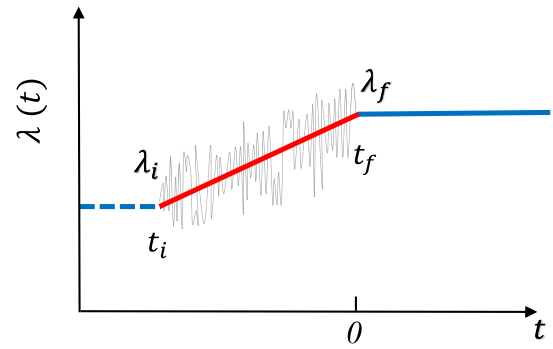

FIG. 1. Illustration of a linear ramped quench (red color). Here, $\lambda(t)$ is the time-dependent parameter in Hamiltonian, λ_i and λ_f its initial and final values, and t_i and $t_f = 0$ the corresponding times. The wavy gray oscillations exhibit the presence of noise.

Summing over the contributions from all modes and replacing summation by the integral in the thermodynamic limit, one gets [116–118]

$$g(t) = \frac{-1}{2\pi}\int_0^\pi \ln\left(1 + 4p_k(p_k - 1)\sin^2\left(\frac{\epsilon_{k,2}^f - \epsilon_{k,1}^f}{2}\right)t\right)dk, \quad (3)$$

where t is measured from the instant the final state, $|\psi_k^f\rangle$, is reached at the end of the ramped quench (Fig. 1). The nonanalyticities in $g(t)$ appear at the values of the real time t_n^*s given by

$$t_n^* = \frac{\pi}{\left(\epsilon_{k^*,2}^f - \epsilon_{k^*,1}^f\right)}(2n+1). \quad (4)$$

These are the critical times for the DQPTs, with k^* the mode at which the argument of the logarithm in Eq. (3) vanishes for $|u_{k^*}|^2 = p_{k^*} = 1/2$.

For the case $\epsilon_{k,2}^f = -\epsilon_{k,1}^f = \epsilon_k^f$, Eq. (4) is simplified to

$$t_n^* = t^*\left(n + \frac{1}{2}\right), \quad t^* = \frac{\pi}{\epsilon_{k^*}^f}. \quad (5)$$

B. Dynamical topological order parameter

The dynamical topological order parameter is introduced to represent the topological characteristic associated with DQPTs [90]. The DTOP displays integer (quantized) values as a function of time and its unit magnitude jumps at the time of DQPTs reveal the topological aspect of DQPT [90,119,120].

The dynamical topological order parameter is defined as [90]

$$N_w(t) = \frac{1}{2\pi}\int_0^\pi \frac{\partial\phi^G(k,t)}{\partial k}\mathrm{d}k, \quad (6)$$

where the geometric phase $\phi^G(k,t)$ is extracted from the total phase $\phi(k,t)$ by subtracting the dynamical phase $\phi^D(k,t)$: $\phi^G(k,t) = \phi(k,t) - \phi^D(k,t)$. The total phase $\phi(k,t)$ is the phase factor of Loschmidt amplitude in its polar coordinate representation, i.e., $\mathcal{L}_k(t) = |\mathcal{L}_k(t)|e^{i\phi(k,t)}$, and $\phi^D(k,t) = -\int_0^t\langle\psi_k^f(t')|H(k,t')|\psi_k^f(t')\rangle dt'$, in which $\phi(k,t)$

and $\phi^D(k,t)$, for the two level system can be calculated as follows [116,117]

$$\phi(k,t) = \tan^{-1}\left(\frac{-|u_k|^2 \sin\left(2\epsilon_k^f t\right)}{|v_k|^2 + |u_k|^2 \cos\left(2\epsilon_k^f t\right)}\right),$$

$$\phi^D(k,t) = -2|u_k|^2 \epsilon_k^f t,$$

so that [116,117]

$$\phi_k^G = \tan^{-1}\left(\frac{-|u_k|^2 \sin\left(2\epsilon_k^f t\right)}{|v_k|^2 + |u_k|^2 \cos\left(2\epsilon_k^f t\right)}\right) + 2|u_k|^2 \epsilon_k^f t. \quad (7)$$

In the following we will study the DQPTs in the long-range pairing Kitaev model following the noiseless and noisy ramped quench and the corresponding topological properties (DTOP).

III. MODEL AND EXACT SOLUTION

Recently, an extension of the Kitaev model [121], which describes the algebraic decay of the tunneling and/or pairing terms has been intensively investigated [12,13,122–124]. This model describes experimental realizations of long-range topological superconductors [125,126]. It has been shown that the phase diagram is modified in the presence of the long-range interactions [13,123]. Moreover, this model exhibits algebraically localized edge states and an algebraic closing of the energy gap [13,123]. However, when the pairing and tunneling terms are isotropic, exponential localization is recovered independent of the power-law exponent, as long as it is larger than unity [12,123].

In this paper, we investigate how the noise affects features of the long-range interaction in the long-range pairing Kitaev model. Representing fermionic annihilation (creation) operators as $c_n(c_n^\dagger)$, the Hamiltonian of the long-range pairing Kitaev model with linear time-dependent chemical potential is given as

$$H = -w\sum_{n=1}^{N}(c_n^\dagger c_{n+1} + \text{H.c.}) - \mu(t)\sum_{n=1}^{N}\left(c_n^\dagger c_n - \frac{1}{2}\right) + \frac{\Delta}{2}\sum_{n,\ell} d_\ell^{-\alpha}(c_n c_{n+\ell} + c_{n+\ell}^\dagger c_n^\dagger), \quad (8)$$

where w denotes the hopping strength of the fermionic particles between adjacent lattice sites, Δ is the strength of the superconducting pairing term that decays with distance l in a power-law fashion characterized by exponent α, and the on-site time-dependent chemical potential $\mu(t) = \mu_f + vt$ changes from the initial value μ_i at time $t = t_i < 0$ to the final values μ_f at $t = t_f = 0$ with sweep velocity v. The effective distance d_ℓ, between two sites denoted by n and $n+\ell$ on the closed ring with N sites, is given by the function $d_\ell = \min(\ell, N-\ell)$.

In the presence of the long-range pairing, the Hamiltonian Eq. (8) is exactly solvable in the momentum space [13]. Introducing the Nambu spinor $\Gamma_{k_m}^\dagger = (c_{k_m}^\dagger,\ c_{-k_m})$, the Fourier transformed Hamiltonian can be expressed as the sum of independent terms acting in the two-dimensional Hilbert space generated by k

$$\mathcal{H}(t) = \frac{1}{2}\sum_{m=1}^{N/2}\Gamma_{k_m}^\dagger H_{k_m}^{(0)}(t)\Gamma_{k_m}, \quad (9)$$

where $H_{k_m}^{(0)}(t)$ [the superscript in $H_{k_m}^{(0)}(t)$ is introduced to denote noise-free driving] is given by

$$H_{k_m}^{(0)}(t) = \begin{pmatrix} -[2w\cos k_m + \mu(t)] & i\Delta f_\alpha(k_m) \\ -i\Delta f_\alpha(k_m) & [2w\cos k_m + \mu(t)] \end{pmatrix}, \quad (10)$$

where $f_\alpha(k_m) = \sum_{\ell=1}^{N-1}\sin(k_m\ell)/d_\ell^\alpha$ is the Fourier transform of the superconducting gap term and $k_m = (2m-1)\pi/N$, $m = 1, 2, \cdots N/2$. In the thermodynamic limit $N \to \infty$, when k_m gets continuous values, the function $f_\alpha(k_m)$, is described as $f_\alpha^\infty(k) = -\frac{i}{2}[\mathbf{Li}_\alpha(e^{ik}) - \mathbf{Li}_\alpha(e^{-ik})]$ with $\mathbf{Li}_\alpha(z) = \sum_{\ell=1}^{\infty} z^\ell/\ell^\alpha$ being the polylogarithmic function of z that vanishes in the limit $k \to 0$ and $k \to \pi$ for $\alpha > 1$. When $\alpha < 1$ the polylogarithmic function only vanishes in the limit $k \to \pi$.

In the limit of $\alpha \to \infty$, the model reduces to that of the short-range Kitaev chain with only nearest-neighbor pairing, which is exactly solvable and its topological properties were unraveled by Kitaev [121]. In this limit, for time-independent chemical potential $\mu(t) = \mu$ and $w = 1$, the time-independent Hamiltonian undergoes topological quantum phase transitions at $\mu_c = \pm 2$, where the energy gap closes at $k = 0, \pi$ [121]. For $\alpha > 1$ the phase diagram and the topological properties of the long-range pairing Kitaev chain are identical to that of a short-range Kitaev chain (Fig. 2). However, as α approaches 1, the bulk gradually starts becoming gapped near $\mu = -2$ and for $\alpha < 1$, $\mu = -2$ no longer remains a critical point [13].

In the time-dependent case $\mu(t) = \mu_f + vt$, the instantaneous eigenvalues and eigenvectors of time dependent

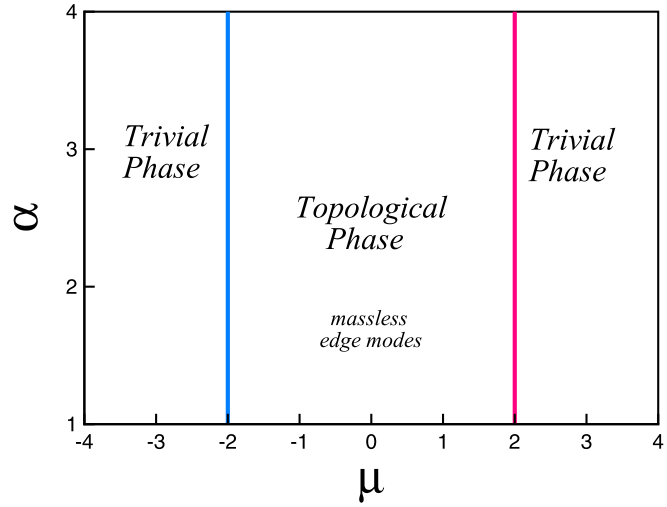

FIG. 2. Phase diagram of the long-range pairing Kitaev chain in the $\mu - \alpha$ plane for $\alpha > 1$.

Hamiltonian Eq. (8), are given by

$$\varepsilon_{k_m}^{\pm} = \pm\varepsilon_{k_m} = \pm\sqrt{h_z^2(k_m,t)+h_{xy}^2(k_m)},$$
$$\left|\chi_{k_m}^{-}(t)\right\rangle = \cos\left(\frac{\theta_{k_m}(t)}{2}\right)|\uparrow\rangle - i\sin\left(\frac{\theta_{k_m}(t)}{2}\right)|\downarrow\rangle,$$
$$\left|\chi_{k_m}^{+}(t)\right\rangle = -i\sin\left(\frac{\theta_{k_m}(t)}{2}\right)|\uparrow\rangle + \cos\left(\frac{\theta_{k_m}(t)}{2}\right)|\downarrow\rangle, \quad (11)$$

where,

$$\cos\left(\frac{\theta_{k_m}(t)}{2}\right) = \frac{\varepsilon_{k_m} - h_z(k_m,t)}{\sqrt{2\varepsilon_{k_m}\left[\varepsilon_{k_m} - h_z(k_m,t)\right]}},$$

$$\sin\left(\frac{\theta_{k_m}(t)}{2}\right) = \frac{h_{xy}(k_m)}{\sqrt{2\varepsilon_{k_m}\left[\varepsilon_{k_m} - h_z(k_m,t)\right]}},$$

with $h_{xy}(k_m) = \Delta f_\alpha(k_m)$, and $h_z(k_m,t) = 2w\cos(k_m) + \mu(t)$, and $|\chi_{k_m,t}^{\pm}\rangle$ are the adiabatic basis of the system.

In such a case, if the system is prepared in its ground state at $t_i \to -\infty$ ($\mu_i \ll \mu_c = -2$), the probability that the kth mode is found in the upper level at t is given as (see Appendix)

$$p_k = e^{-\pi\gamma^2/4}\left|U_{22}\cos\left(\frac{\theta_{k_m}(t)}{2}\right) - \frac{\gamma e^{-i\pi/4}}{\sqrt{2}}U_{12}\sin\left(\frac{\theta_{k_m}(t)}{2}\right)\right|^2, \quad (12)$$

with $U_{22} = D_\nu(x)$, $U_{12} = D_{\nu-1}(x)$, where, $D_\nu(x)$ is the parabolic cylinder function [127,128], $\gamma = \Delta f_\alpha(k_m)/\sqrt{2v}$, $\nu = i\gamma^2/2$, $x = 2e^{i3\pi/4}\sqrt{v}\tau_k$, and $\tau_k = [(\mu_f + vt)/2 + w\cos(k)]/v$.

IV. NOISELESS NUMERICAL RESULTS

In this section, we report the results of our numerical simulations, based on an analytical approach, to investigate the dynamics of the model using the notion of DQPTs. To this end, we consider the linear quenching of the chemical potential $\mu(t) = \mu_f + vt$, changes from initial value $\mu_i \to -\infty$, where the system is prepared in its ground state, to various final values $\mu_f = 1, 1.95, 4$ at $t_f = 0$. In addition, to better understand the effect of long-range pairing on the dynamics of system after the ramp quench, we will focus only on the case $\alpha > 1$ where the location of the critical points in the parameter space is not altered by varying α.

1. Quench across a single critical point

For the ramped quench, which crosses the single critical point $\mu_c = -2$ at $k = 0$, the excitation probability after quench is k dependent. As expected, when the system is driven across the critical point, the system undergoes nonadiabatic evolution due to the gap closing and thus the transition probability is maximum at the gap closing mode $k = 0$. However, away from the gap closing mode the system evolves adiabatically due to the nonzero energy gap and can be shown that $p_{k\to\pi} \to 0$. Considering these two limiting cases, and also continuity of the transition probability as a function of k in the thermodynamic limit, imply that there should exist a critical mode k^* at which $p_{k^*} = 1/2$ and consequently DQPTs occur. The transition probability has been plotted versus k in Figs. 3(a) and 3(b) for $\mu_f = 1, 1.95$ for different sweep velocities as the ramped quench crosses the single critical point $\mu_c = -2$. Since the quench crosses the critical point, the excitation probability takes its maximum value $p_k = 1$ at $k = 0$, while it is negligible away from the gap closing mode ($k \to \pi$). From these observations, it is straightforward to conclude that there is always a critical momentum k^* and hence those of t_n^*, related through Eq. (6). Interestingly, we observed that there exists a region in the parameter space v-α where the system encompasses three distinct critical modes k^* for which $p_{k^*} = 1/2$, even though the system is quenched across a single QCP. In such a case, the system displays three different critical time scales t^* as obtained from Eq. (6). While in the short-range case [80,117] the system contains only a single critical mode following a quench across a single QCP. In Fig. 3(c), we have plotted a phase diagram in v-α plane for $\mu_f = 1$, and $\mu_f = 1.95$ in which region with three critical modes (TCMs) separated from the regions with single critical mode (SCM). On the phase boundary separating these two regions, there are two values of k^* with $p_{k^*} = 1/2$. As seen, the width of TCMs region shrinks and vanishes as α increases and also as μ_f decreases. The numerical results show that the threshold values of μ_f above which TCMs region appears is $\mu_f \geqslant -0.1$. In other words, the exponent α has a critical value $\alpha_c(v, \mu_f)$ above which the dynamical behavior of the system is similar to that of the short-range system. Consequently, our findings confirm that the appearance of TCMs region is indeed an artifact of the long-range pairing nature of the Hamiltonian.

The dynamical free energy $g(t)$ and DTOP (N_w) of the model have been depicted in Figs. 3(d)–3(f) for the quench across a single critical point [corresponding to Fig. 3(b)], for different sweep velocities $v = 2.5, 9$ and $v = 6$, respectively. In Figs. 3(d) and 3(f) the system is in SCM region, where it encompasses a single critical time scale t^*. Although the cusps in $g(t)$ are not discernible but the quantization and jumps in the associated DTOP are clearly visible as an indicator of DQPTs. The observed oscillation in the dynamical free energy seems to be the natural behavior, which results from the unitary time evolution of the postquench ground state in terms of the Hamiltonian's eigenstates. The behavior of DTOP, i.e., whether $N_w(t)$ would jump or drop, can be predicted by the slope of p_k at the critical momentum k^* [positive (negative) slop results jump (drop)] [108,117]. Appearing successive jumps or drops in $N_w(t)$ indicate that the system has only a single critical mode, while the presence of both jump and drop in DTOP curve implies that the system has at least two critical modes as seen in Fig. 3(e). As seen, uninterrupted jumps in Figs. 3(d) and 3(f) reveal that the system is in SCM region while two successive jumps and then drop of N_w(t) in Fig. 3(e) points the existence of three different critical modes in accordance with p_k [Fig. 3(b)], which shows that the system is in TCMs region.

2. Quench across two critical points

Performing a quench across both equilibrium critical points $\mu_c = \pm 2$ shows new features. In these cases, the chemical potential is swept from one trivial (nontopological) phase to

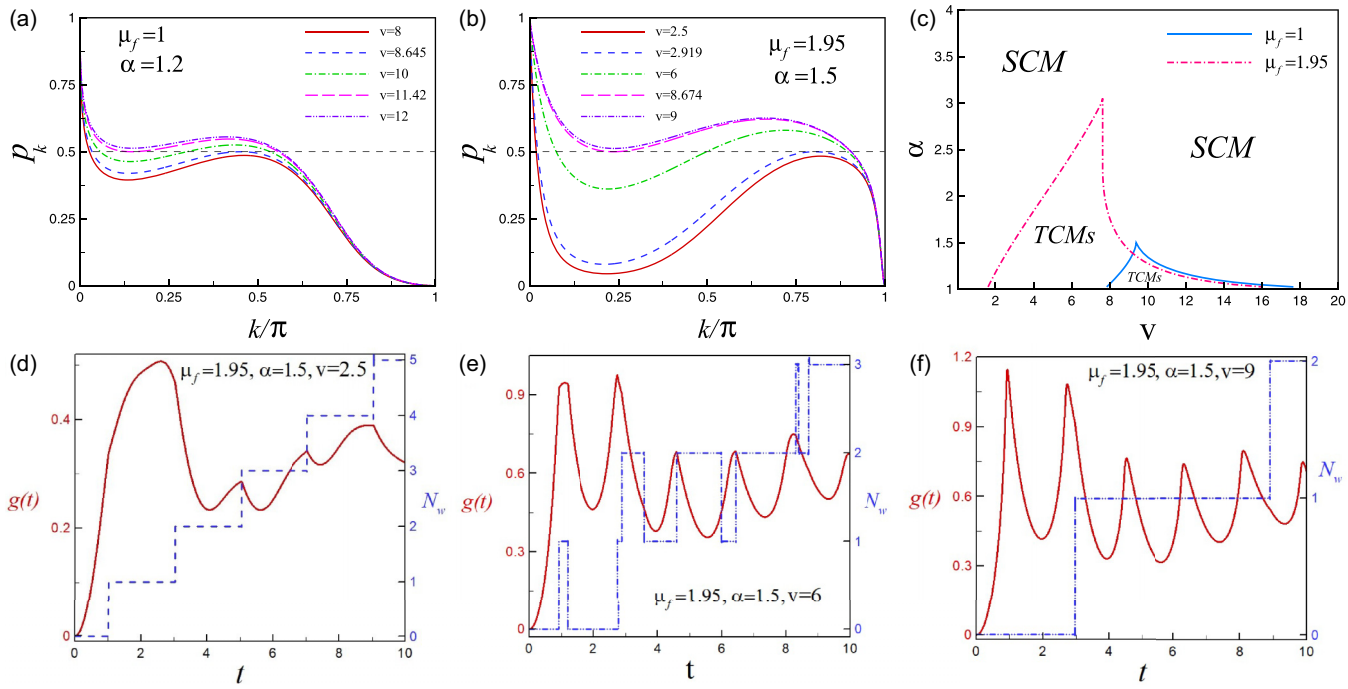

FIG. 3. Probability p_k for finding the system with momentum k in the upper level for the noiseless ramped across the single critical point $\mu_c = -2$, for different sweep velocities, (a) for $\alpha = 1.2$ and $\mu_f = 1$, (b) for $\alpha = 1.5$ and $\mu_f = 1.95$. (c) The phase diagram of the model in v-α plane for a noiseless quench that crosses the single critical point $\mu_c = -2$ for $\mu_f = 1$ (solid line) and $\mu_f = 1.95$ (dashed-dotted line). The dynamical free energy $g(t)$ and its associated dynamical topological order parameter $N_w(t)$ for a noiseless quench across the single critical point corresponding to Fig. 3(b) for (d) $v = 2.5$, (e) $v = 6$, and (f) $v = 9$.

another one, and it is not expected to result in DQPTs when the quench is sudden [48,117,118]. For a quench crossing both critical points, as expected, the nonadiabatic evolution of the system at gap closing modes $k = 0, \pi$, leads to maximum transition probability, i.e., $p_{k=0,\pi} = 1$.

However, the minimum of p_k, occurs at the maximum energy gap mode at $k = \pi/2$, which is the farthest mode from the gap closing mode. Since, the maximum value of transition probability $p_{k=0,\pi} = 1$ is greater than $1/2$, the appearance of DQPTs requires the condition that the minimum value of transition probability becomes less than $1/2$. As the system changes adiabatically at the gapped mode for small sweep velocity, making the quench sufficiently slow ($v < v_c$) ensures that the minimum excitation probability is smaller than $1/2$, which sets a succession of DQPTs. In Fig. 4(a) the transition probability has been shown versus k for a quench that crosses two critical points (i.e. $\mu_f = 4$) for the exponent $\alpha = 1.5$. As predicted, $p_{k=0,\pi} = 1$ and the minimum of p_k away from the critical modes is less than $1/2$ for the small sweep velocity ($v < v_c = 9.566$). In such a case, there is two critical modes k^*_β and k^*_γ at which $p_{k^*_{\beta,\gamma}} = 1/2$ yields a sequence of DQPTs at the corresponding critical times $t^*_n = t^*_{n,\beta}, t^*_{n,\gamma}, n = 0, 1, \ldots$. Furthermore, the minimum of p_k becomes greater than $1/2$ for a sweep velocity greater than the critical sweep

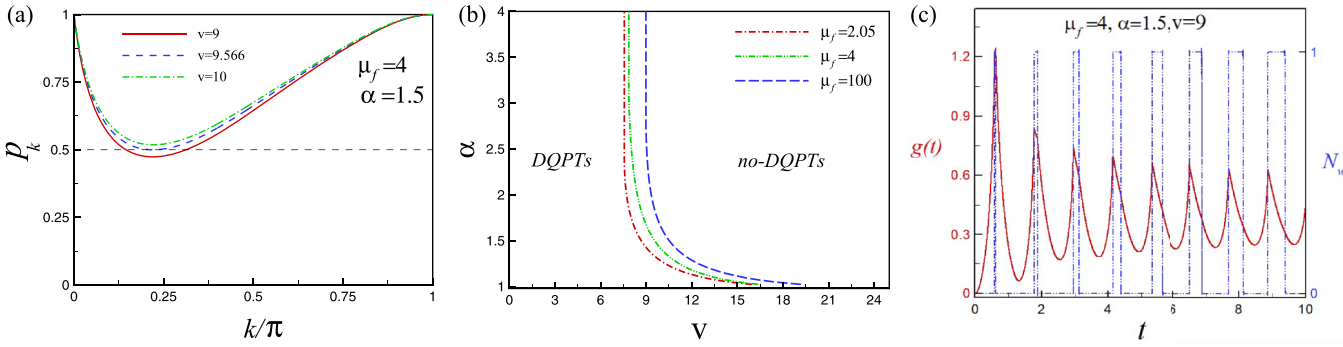

FIG. 4. (a) Probability of the excitation for noiseless ramped quench, which crosses two critical points $\mu_c = \pm 2$, for different sweep velocities, $\alpha = 1.5$ and $\mu_f = 4$. (b) The phase diagram of the model in v-α plane for a noiseless quench that crosses two critical points $\mu_c = \pm 2$ for $\mu_f = 2.05$ (dashed-dotted line), $\mu_f = 4$ (dashed-dotted-dotted line), and $\mu_f = 4$ (dashed line). (c) The dynamical free energy $g(t)$ and the associated dynamical topological order parameter $N_w(t)$ for a noiseless quench crosses two critical points corresponding to Fig. 4(a) for $v = 9$.

velocity $v = 10 > v_c = 9.566$, thus blocking the appearance of DQPTs.

The phase diagram of the model for a quench crossing two critical points, has been illustrated in Fig. 4(b) for different values of $\mu_f = 2.05, 4$ and $\mu_f = 100$ where the region marked "DQPTs" support aperiodic sequences of DQPTs. As seen, the critical sweep velocity v_c decreases by increasing the exponent α and v_c is equivalent to the that of short-range pairing system for $\alpha > 2$.

Figure 4(c) shows the dynamical free energy and DTOP for a quench crossing two critical points $\mu_c = -2$ and $\mu_f = 2$. Cusps in $g(t)$ and quantizations in the associated DTOP are clearly visible as an indicator of DQPTs. As observed, DTOP oscillates between 0 and 1, which indicates that the corresponding p_k contains two critical modes with different slopes [Fig. 4(a)].

V. NOISY RAMP QUENCH

As mentioned the noises are ubiquitous and indispensable in any physical system. Specifically, when energy is transferred into or out of an otherwise isolated system via a quench in the laboratory, there will inevitably be time-dependent fluctuations (noise) in this transfer. In this section we investigate the effects of noise on the dynamical phase diagram of the long-range pairing Kitaev model. For this purpose, we add a noise to the time-dependent chemical potential $\mu(t) = \mu_f + vt + R(t)$, where $R(t)$ is a random fluctuation confined to the ramp interval $[t_i, t_f = 0[$, with vanishing mean, $\langle R(t)\rangle = 0$. We use white noise with Gaussian two-point correlations $\langle R(t)R(t')\rangle = \xi^2\delta(t - t')$, where ξ characterizes the strength of the noise (ξ^2 has units of time). White noise is approximately equivalent to fast colored noise with exponentially decaying two-point correlations (Ornstein-Uhlenbeck process) [115]. In the presence of noise the transition probability is obtained by numerically solving the exact master equation [129–132] for the averaged density matrix $\rho_{k_m}(t)$ of the noisy system

$$\frac{d}{dt}\rho_{k_m}(t) = -i\big[H^{(0)}_{k_m}(t), \rho_{k_m}(t)\big] - \frac{\xi^2}{2}\big\{H_1, \big[H_1, \rho_{k_m}(t)\big]\big\}, \tag{13}$$

where $H^{(0)}_{k_m}(t)$ is the noise-free Hamiltonian while $R(t)H_1 = -R(t)\sigma^z$ expresses the noisy part for the full Hamiltonian $H^{(\xi)}_{k_m}(t) = H^{(0)}_{k_m}(t) + R(t)H_1$. The master equation, Eq. (12), is solved within the quench interval $t \in [t_i, 0]$.

The transition probability p_k in the presence of the noise is given by

$$p_{k_m} = \big\langle \chi^+_{k_m}(t_f)\big|\rho_{k_m}(t_f)\big|\chi^+_{k_m}(t_f)\big\rangle.$$

As a result, the dynamical phase diagram of the model is characterized by the interplay of two competing effects: (i) The nontrivial excitation resulting from the long-range pairing and (ii) the accumulation of noise-induced excitations during the evolution. Moreover, we expect that the nonadiabaticity by large values of the sweep velocity gives less time for the noise to become effective. Our numerical simulation, which is based on the exact master equation reveals that the main effect of noise is to shift the critical mode yielding the succession of DQPTs and a shift on the phase boundaries. In addition, the numerical results uncover that the noise contributions diminish the long-range pairing dynamics.

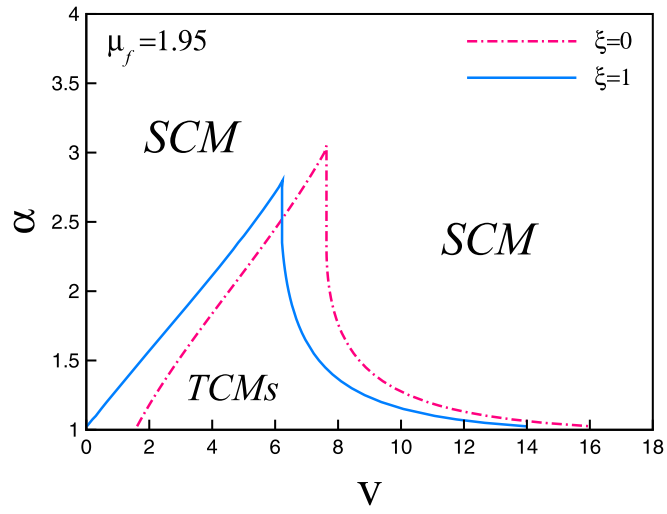

FIG. 5. The phase diagram of the underlying model in v-α plane for a noiseless and noisy quench that crosses a single critical point $\mu_c = 2$ for $\mu_f = 1.95$. The dashed-dotted line represents the boundary between TCMs and SCM region for the noiseless case and solid line displays the boundaries for the noise intensity $\xi = 1$.

The phase diagram of the model in the absence and presence of the noise ($\xi = 0, 1$) has been plotted in Fig. 5 for a quench across the single critical point for $\mu_f = 1.95$. As seen, the TCMs boundaries change in the presence of the noise. Moreover, the width of TCMs region shrinks rapidly as exponent α increases. In addition, the borders between TCMs and SCM regions change less for large values of sweep velocity, which corresponds to our anticipation. In other words, the noise weakens the effect of long-range pairing on the dynamical phase diagram.

Figure 6 depicts the border between DQPTs and no-DQPTs regions for both noiseless $\xi = 0$ and noisy $\xi = 1$ cases, for a ramped quench that crosses two critical points for $\mu_f = 4$. As indicated, the critical sweep velocity above which the DQPT is wiped out decreases in the presence of the noise even for large values of α, where the critical values of the sweep velocity is the same as that of short-range pairing case. Moreover, the border undergoes more changes for the smaller sweep velocities than the larger sweep velocities. However, the changes are constant for $\alpha > 2$, where the dynamics is the same as that of the short-range pairing case. The numerical results show that the changes in the border of different regions in the phase diagram of both ramped quench cases (Figs. 5 and 6) decrease by decreasing the noise strength, as anticipated.

VI. SUMMARY AND DISCUSSION

In this paper, we have studied the nonequilibrium dynamics of the long-range pairing Kitaev model ($\alpha > 1$) with noiseless and noisy linear time-dependent chemical potential. For a noiseless quench across one of the equilibrium quantum critical points ($\mu_c = -2$), we find that the dynamical phase diagram in v-α plane is classified into two regions,

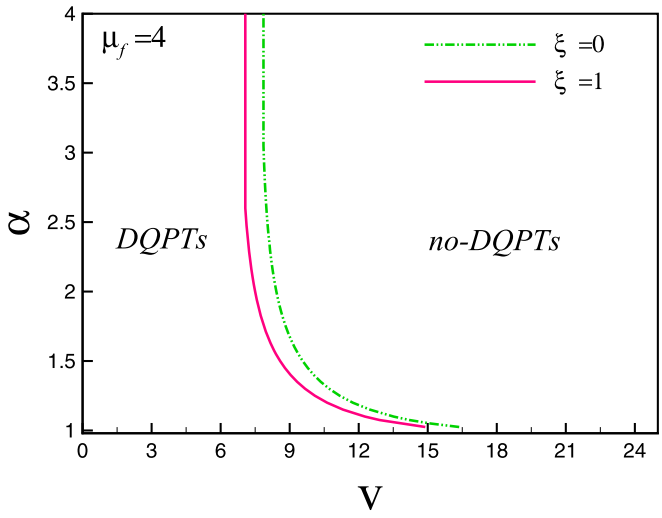

FIG. 6. The v-α phase diagram of the model for a noiseless and noisy quench, which crosses two critical points $\mu_c = \pm 2$ for $\mu_f = 4$. The dashed-dotted-dotted line shows the boundary between DQPTs and no-DQPTs regions for the noiseless case and solid line represent the corresponding border for the noise intensity $\xi = 1$.

the three critical modes and the single critical mode regions. The three critical modes region is the result of the long-range pairing, in contrast to the short-range Kitaev model, which shows a single critical mode for a noiseless quench across a single critical point. The three critical modes region shrinks and disappears as the exponent α increases. In addition, the numerical results show that appearance of the three critical modes region depends on the final values of the chemical potential. The lower bond of the chemical potential above which three critical modes region emerges is $\mu_f = -0.1$ and the upper bound is the next critical point, i.e., $-0.1 \leqslant \mu_f < 2$. Moreover, the exponent α has a critical value $\alpha_c(v, \mu_f)$ above which the dynamical behavior of the long-range pairing system is similar to that of the short-range system. Consequently, our finding confirms that the appearance of TCMs region is indeed an outcome of the long-range pairing nature of the Hamiltonian.

Further, for a noiseless ramped quench that crosses two critical points, the critical sweep velocity above which the dynamical quantum phase transition is wiped out for long-range pairing, is larger than that of the short-range pairing case. The critical sweep velocity decreases by increasing the exponent α of long-range pairing and saturates to the critical sweep velocity of the short-range pairing case beyond $\alpha = 2$.

The boundaries between different regions in both cases of the ramped quench, are changed in the presence of the Gaussian white noise. The three critical modes region for the quench that crosses the single critical point shrinks faster in the presence of noise by increasing α. Moreover, for the ramped quench, which crosses two critical points, the critical sweep velocity above which the dynamical quantum phase transition disappears reduces by adding noise. The numerical results exhibit that the system is affected less at the large sweep velocities. In summary, the noise has destructive effects on the long-range pairing features.

The case of $\alpha < 1$ hosts massive edge modes for the open boundary condition, which is not our case. However, the study of a system with massive edge modes could be an interesting issue for further investigations.

APPENDIX: TIME-DEPENDENT SCHRÖDINGER EQUATION IN THE DIABATIC BASIS

The time-dependent Schrödinger equation of Hamiltonian in Eq. (8) is given by

$$i\frac{d}{dt}\begin{pmatrix} a_1(t) \\ a_2(t) \end{pmatrix} = \begin{pmatrix} -h_z(k,t) & ih_{x,y} \\ -ih_{x,y} & h_z(k,t) \end{pmatrix}\begin{pmatrix} a_1(t) \\ a_2(t) \end{pmatrix}, \quad \text{(A1)}$$

where $h_z(k,t) = [2w\cos k_m + \mu(t)]$, $h_{x,y} = i\Delta f_\alpha(k_m)$ and $a_1(t)$, $a_2(t)$ are the coefficients, which define the quantum state in the diabatic bases. The time-dependent Schrödinger Eq. (A1) is mapped to the time-dependent Schrödinger equation of Landau-Zener problem [133,134] by performing $\pi/2$ rotation around the z axes and defining the new time scale $\tau_k = [\mu_f + vt + 2w\cos(k)]/2v$,

$$i\frac{d}{d\tau_{k_m}}\begin{pmatrix} a_1(\tau_{k_m}) \\ a_2(\tau_{k_m}) \end{pmatrix} = \begin{pmatrix} -2v\tau_{k_m} & \Delta f_\alpha(k_m) \\ \Delta f_\alpha(k_m) & 2v\tau_{k_m} \end{pmatrix}\begin{pmatrix} a_1(\tau_{k_m}) \\ a_2(\tau_{k_m}) \end{pmatrix}. \quad \text{(A2)}$$

The Landau-Zener problem is exactly solvable as explained in Refs. [133,134] and the transition probability is given by Eq. (12).

[1] D. J. Thouless, Long-range order in one-dimensional Ising systems, Phys. Rev. **187**, 732 (1969).

[2] M. E. Fisher, S.-k. Ma, and B. G. Nickel, Critical exponents for long-range interactions, Phys. Rev. Lett. **29**, 917 (1972).

[3] A. Dutta and J. K. Bhattacharjee, Phase transitions in the quantum Ising and rotor models with a long-range interaction, Phys. Rev. B **64**, 184106 (2001).

[4] E. Luijten and H. Meßingfeld, Criticality in one dimension with inverse square-law potentials, Phys. Rev. Lett. **86**, 5305 (2001).

[5] M. Van Regemortel, D. Sels, and M. Wouters, Information propagation and equilibration in long-range Kitaev chains, Phys. Rev. A **93**, 032311 (2016).

[6] D. Giuliano, S. Paganelli, and L. Lepori, Current transport properties and phase diagram of a Kitaev chain with long-range pairing, Phys. Rev. B **97**, 155113 (2018).

[7] F. Ares, J. G. Esteve, F. Falceto, and A. R. de Queiroz, Entanglement entropy in the long-range Kitaev chain, Phys. Rev. A **97**, 062301 (2018).

[8] M. Benito, A. Gómez-León, V. M. Bastidas, T. Brandes, and G. Platero, Floquet engineering of long-range p-wave superconductivity, Phys. Rev. B **90**, 205127 (2014).

[9] G. Francica and L. Dell'Anna, Correlations, long-range entanglement, and dynamics in long-range Kitaev chains, Phys. Rev. B **106**, 155126 (2022).

[10] S. Mondal, S. Bandyopadhyay, S. Bhattacharjee, and A. Dutta, Detecting topological phase transitions through entanglement

between disconnected partitions in a Kitaev chain with long-range interactions, Phys. Rev. B **105**, 085106 (2022).
[11] R. G. Dias and A. M. Marques, Long-range hopping and indexing assumption in one-dimensional topological insulators, Phys. Rev. B **105**, 035102 (2022).
[12] S. B. Jäger, L. Dell'Anna, and G. Morigi, Edge states of the long-range Kitaev chain: An analytical study, Phys. Rev. B **102**, 035152 (2020).
[13] D. Vodola, L. Lepori, E. Ercolessi, A. V. Gorshkov, and G. Pupillo, Kitaev chains with long-range pairing, Phys. Rev. Lett. **113**, 156402 (2014).
[14] U. Bhattacharya and A. Dutta, Topological footprints of the Kitaev chain with long-range superconducting pairings at a finite temperature, Phys. Rev. B **97**, 214505 (2018).
[15] P. Schauß, M. Cheneau, M. Endres, T. Fukuhara, S. Hild, A. Omran, T. Pohl, C. Gross, S. Kuhr, and I. Bloch, Observation of spatially ordered structures in a two-dimensional Rydberg gas, Nature (London) **491**, 87 (2012).
[16] J. W. Britton, B. C. Sawyer, A. C. Keith, C.-C. J. Wang, J. K. Freericks, H. Uys, M. J. Biercuk, and J. J. Bollinger, Engineered two-dimensional Ising interactions in a trapped-ion quantum simulator with hundreds of spins, Nature (London) **484**, 489 (2012).
[17] R. Islam, C. Senko, W. C. Campbell, S. Korenblit, J. Smith, A. Lee, E. E. Edwards, C.-C. J. Wang, J. K. Freericks, and C. Monroe, Emergence and frustration of magnetism with variable-range interactions in a quantum simulator, Science **340**, 583 (2013).
[18] P. Richerme, Z.-X. Gong, A. Lee, C. Senko, J. Smith, M. Foss-Feig, S. Michalakis, A. V. Gorshkov, and C. Monroe, Non-local propagation of correlations in quantum systems with long-range interactions, Nature (London) **511**, 198 (2014).
[19] C. Monroe, W. C. Campbell, L.-M. Duan, Z.-X. Gong, A. V. Gorshkov, P. W. Hess, R. Islam, K. Kim, N. M. Linke, G. Pagano, P. Richerme, C. Senko, and N. Y. Yao, Programmable quantum simulations of spin systems with trapped ions, Rev. Mod. Phys. **93**, 025001 (2021).
[20] I. Bloch, J. Dalibard, and S. Nascimbene, Quantum simulations with ultracold quantum gases, Nat. Phys. **8**, 267 (2012).
[21] M. Dupont and J. E. Moore, Quantum criticality using a superconducting quantum processor, Phys. Rev. B **106**, L041109 (2022).
[22] T. Langen, R. Geiger, and J. Schmiedmayer, Ultracold atoms out of equilibrium, Annu. Rev. Condens. Matter Phys. **6**, 201 (2015).
[23] A. D. King, S. Suzuki, J. Raymond, A. Zucca, T. Lanting, F. Altomare, A. J. Berkley, S. Ejtemaee, E. Hoskinson, S. Huang *et al.*, Coherent quantum annealing in a programmable 2,000 qubit Ising chain, Nat. Phys. **18**, 1324 (2022).
[24] A. Keesling, A. Omran, H. Levine, H. Bernien, H. Pichler, S. Choi, R. Samajdar, S. Schwartz, P. Silvi, S. Sachdev *et al.*, Quantum kibble–zurek mechanism and critical dynamics on a programmable Rydberg simulator, Nature (London) **568**, 207 (2019).
[25] A. Polkovnikov, K. Sengupta, A. Silva, and M. Vengalattore, Colloquium: Nonequilibrium dynamics of closed interacting quantum systems, Rev. Mod. Phys. **83**, 863 (2011).
[26] J. Dziarmaga, Dynamics of a quantum phase transition: Exact solution of the quantum Ising model, Phys. Rev. Lett. **95**, 245701 (2005).
[27] A. Francuz, J. Dziarmaga, B. Gardas, and W. H. Zurek, Space and time renormalization in phase transition dynamics, Phys. Rev. B **93**, 075134 (2016).
[28] X. Yang and Z. Cai, Dynamical transitions and critical behavior between discrete time crystal phases, Phys. Rev. Lett. **126**, 020602 (2021).
[29] D. A. Abanin, E. Altman, I. Bloch, and M. Serbyn, Colloquium: Many-body localization, thermalization, and entanglement, Rev. Mod. Phys. **91**, 021001 (2019).
[30] U. Mishra, R. Prabhu, A. Sen (De), and U. Sen, Tuning interaction strength leads to an ergodic-nonergodic transition of quantum correlations in the anisotropic heisenberg spin model, Phys. Rev. A **87**, 052318 (2013).
[31] T. Chanda, T. Das, D. Sadhukhan, A. K. Pal, A. Sen (De), and U. Sen, Static and dynamical quantum correlations in phases of an alternating-field XY model, Phys. Rev. A **94**, 042310 (2016).
[32] N. Awasthi, S. Bhattacharya, A. Sen (De), and U. Sen, Universal quantum uncertainty relations between nonergodicity and loss of information, Phys. Rev. A **97**, 032103 (2018).
[33] M. Heyl, A. Polkovnikov, and S. Kehrein, Dynamical quantum phase transitions in the transverse-field Ising model, Phys. Rev. Lett. **110**, 135704 (2013).
[34] M. Heyl, Dynamical quantum phase transitions: A review, Rep. Prog. Phys. **81**, 054001 (2018).
[35] R. Jafari, H. Johannesson, A. Langari, and M. A. Martin-Delgado, Quench dynamics and zero-energy modes: The case of the Creutz model, Phys. Rev. B **99**, 054302 (2019).
[36] R. Jafari and H. Johannesson, Loschmidt echo revivals: Critical and noncritical, Phys. Rev. Lett. **118**, 015701 (2017).
[37] K. Najafi, M. A. Rajabpour, and J. Viti, Return amplitude after a quantum quench in the XY chain, J. Stat. Mech.: Theory Exp. (2019) 083102.
[38] S. Mukherjee and T. Nag, Dynamics of decoherence of an entangled pair of qubits locally connected to a one-dimensional disordered spin chain, J. Stat. Mech.: Theory Exp. (2019) 043108.
[39] J. M. Zhang and H.-T. Yang, Cusps in the quench dynamics of a bloch state, Europhys. Lett. **114**, 60001 (2016).
[40] M. Serbyn and D. A. Abanin, Loschmidt echo in many-body localized phases, Phys. Rev. B **96**, 014202 (2017).
[41] M. Sadrzadeh, R. Jafari, and A. Langari, Dynamical topological quantum phase transitions at criticality, Phys. Rev. B **103**, 144305 (2021).
[42] C. Y. Wong and W. C. Yu, Loschmidt amplitude spectrum in dynamical quantum phase transitions, Phys. Rev. B **105**, 174307 (2022).
[43] C. Rylands, E. A. Yuzbashyan, V. Gurarie, A. Zabalo, and V. Galitski, Loschmidt echo of far-from-equilibrium fermionic superfluids, Ann. Phys. (NY) **435**, 168554 (2021).
[44] M. Abdi, Dynamical quantum phase transition in Bose-Einstein condensates, Phys. Rev. B **100**, 184310 (2019).
[45] F. Andraschko and J. Sirker, Dynamical quantum phase transitions and the loschmidt echo: A transfer matrix approach, Phys. Rev. B **89**, 125120 (2014).

[46] S. Vajna and B. Dóra, Topological classification of dynamical phase transitions, Phys. Rev. B **91**, 155127 (2015).
[47] C. Karrasch and D. Schuricht, Dynamical phase transitions after quenches in nonintegrable models, Phys. Rev. B **87**, 195104 (2013).
[48] S. Vajna and B. Dóra, Disentangling dynamical phase transitions from equilibrium phase transitions, Phys. Rev. B **89**, 161105(R) (2014).
[49] R. Jafari, Dynamical quantum phase transition and quasi particle excitation, Sci. Rep. **9**, 2871 (2019).
[50] D. Mondal and T. Nag, Anomaly in the dynamical quantum phase transition in a non-Hermitian system with extended gapless phases, Phys. Rev. B **106**, 054308 (2022).
[51] J. J. Mendoza-Arenas, Dynamical quantum phase transitions in the one-dimensional extended fermi–hubbard model, J. Stat. Mech.: Theory Exp. (2022) 043101.
[52] N. Sedlmayr, P. Jaeger, M. Maiti, and J. Sirker, Bulk-boundary correspondence for dynamical phase transitions in one-dimensional topological insulators and superconductors, Phys. Rev. B **97**, 064304 (2018).
[53] N. Sedlmayr, M. Fleischhauer, and J. Sirker, Fate of dynamical phase transitions at finite temperatures and in open systems, Phys. Rev. B **97**, 045147 (2018).
[54] A. Khatun and S. M. Bhattacharjee, Boundaries and unphysical fixed points in dynamical quantum phase transitions, Phys. Rev. Lett. **123**, 160603 (2019).
[55] C. Ding, Dynamical quantum phase transition from a critical quantum quench, Phys. Rev. B **102**, 060409(R) (2020).
[56] A. L. Corps and A. Relaño, Theory of dynamical phase transitions in quantum systems with symmetry-breaking eigenstates, Phys. Rev. Lett. **130**, 100402 (2023).
[57] S. De Nicola, A. A. Michailidis, and M. Serbyn, Entanglement view of dynamical quantum phase transitions, Phys. Rev. Lett. **126**, 040602 (2021).
[58] A. D. Verga, Entanglement dynamics and phase transitions of the floquet cluster spin chain, Phys. Rev. B **107**, 085116 (2023).
[59] L. Rossi and F. Dolcini, Nonlinear current and dynamical quantum phase transitions in the flux-quenched su-schrieffer-heeger model, Phys. Rev. B **106**, 045410 (2022).
[60] N. A. Khan, P. Wang, M. Jan, and G. Xianlong, Anomalous correlation-induced dynamical phase transitions, Sci. Rep. **13**, 9470 (2023).
[61] N. A. Khan, X. Wei, S. Cheng, M. Jan, and G. Xianlong, Dynamical phase transitions in dimerized lattices, Phys. Lett. A **475**, 128880 (2023).
[62] F. A. Wolf, I. P. McCulloch, and U. Schollwöck, Solving nonequilibrium dynamical mean-field theory using matrix product states, Phys. Rev. B **90**, 235131 (2014).
[63] L. Zhou and Q. Du, Non-Hermitian topological phases and dynamical quantum phase transitions: A generic connection, New J. Phys. **23**, 063041 (2021).
[64] T. I. Vanhala and T. Ojanen, Theory of the loschmidt echo and dynamical quantum phase transitions in disordered Fermi systems, Phys. Rev. Res. **5**, 033178 (2023).
[65] D. Mondal and T. Nag, Finite-temperature dynamical quantum phase transition in a non-Hermitian system, Phys. Rev. B **107**, 184311 (2023).
[66] K. Cao, W. Li, M. Zhong, and P. Tong, Influence of weak disorder on the dynamical quantum phase transitions in the anisotropic XY chain, Phys. Rev. B **102**, 014207 (2020).
[67] T. Masłowski and N. Sedlmayr, Dynamical bulk-boundary correspondence and dynamical quantum phase transitions in higher-order topological insulators, Phys. Rev. B **108**, 094306 (2023).
[68] K. Wrześniewski, I. Weymann, N. Sedlmayr, and T. Domański, Dynamical quantum phase transitions in a mesoscopic superconducting system, Phys. Rev. B **105**, 094514 (2022).
[69] A. L. Corps and A. Relaño, Dynamical and excited-state quantum phase transitions in collective systems, Phys. Rev. B **106**, 024311 (2022).
[70] T. Masłowski and N. Sedlmayr, Quasiperiodic dynamical quantum phase transitions in multiband topological insulators and connections with entanglement entropy and fidelity susceptibility, Phys. Rev. B **101**, 014301 (2020).
[71] Y. Zeng, B. Zhou, and S. Chen, Dynamical singularity of the rate function for quench dynamics in finite-size quantum systems, Phys. Rev. B **107**, 134302 (2023).
[72] S. Stumper, M. Thoss, and J. Okamoto, Interaction-driven dynamical quantum phase transitions in a strongly correlated bosonic system, Phys. Rev. Res. **4**, 013002 (2022).
[73] W. C. Yu, P. D. Sacramento, Y. C. Li, and H.-Q. Lin, Correlations and dynamical quantum phase transitions in an interacting topological insulator, Phys. Rev. B **104**, 085104 (2021).
[74] V. Vijayan, L. Chotorlishvili, A. Ernst, S. S. P. Parkin, M. I. Katsnelson, and S. K. Mishra, Topological dynamical quantum phase transition in a quantum skyrmion phase, Phys. Rev. B **107**, L100419 (2023).
[75] Z.-R. Zhu, B. Shao, J. Zou, and L.-A. Wu, Orthogonality catastrophe and quantum speed limit for dynamical quantum phase transition, Physica A: Stat. Mech. Appl. **634**, 129455 (2024).
[76] X.-J. Yu, Dynamical phase transition and scaling in the chiral clock potts chain, Phys. Rev. A **108**, 062215 (2023).
[77] S. M. Bhattacharjee, Complex dynamics approach to dynamical quantum phase transitions: The potts model, Phys. Rev. B **109**, 035130 (2024).
[78] L. G. C. Lakkaraju, S. K. Haldar, and A. Sen (De), Predicting a topological quantum phase transition from dynamics via multisite entanglement, Phys. Rev. A **109**, 022436 (2024).
[79] T. Puskarov and D. Schuricht, Time evolution during and after finite-time quantum quenches in the transverse-field Ising chain, SciPost Phys. **1**, 003 (2016).
[80] S. Zamani, J. Naji, R. Jafari, and A. Langari, Scaling and universality at ramped quench dynamical quantum phase transitions, J. Phys.: Condens. Matter **36**, 355401 (2024).
[81] G. Delfino and M. Sorba, Persistent oscillations after quantum quenches in d dimensions, Nucl. Phys. B **974**, 115643 (2022).
[82] K. Yang, L. Zhou, W. Ma, X. Kong, P. Wang, X. Qin, X. Rong, Y. Wang, F. Shi, J. Gong, and J. Du, Floquet dynamical quantum phase transitions, Phys. Rev. B **100**, 085308 (2019).
[83] S. Zamani, R. Jafari, and A. Langari, Floquet dynamical quantum phase transition in the extended XY model: Nonadiabatic to adiabatic topological transition, Phys. Rev. B **102**, 144306 (2020).

[84] A. Kosior and K. Sacha, Dynamical quantum phase transitions in discrete time crystals, Phys. Rev. A **97**, 053621 (2018).
[85] R. Jafari and A. Akbari, Floquet dynamical phase transition and entanglement spectrum, Phys. Rev. A **103**, 012204 (2021).
[86] A. Kosior, A. Syrwid, and K. Sacha, Dynamical quantum phase transitions in systems with broken continuous time and space translation symmetries, Phys. Rev. A **98**, 023612 (2018).
[87] J. Naji, M. Jafari, R. Jafari, and A. Akbari, Dissipative floquet dynamical quantum phase transition, Phys. Rev. A **105**, 022220 (2022).
[88] R. Jafari, A. Akbari, U. Mishra, and H. Johannesson, Floquet dynamical quantum phase transitions under synchronized periodic driving, Phys. Rev. B **105**, 094311 (2022).
[89] J. Naji, R. Jafari, L. Zhou, and A. Langari, Engineering floquet dynamical quantum phase transitions, Phys. Rev. B **106**, 094314 (2022).
[90] J. C. Budich and M. Heyl, Dynamical topological order parameters far from equilibrium, Phys. Rev. B **93**, 085416 (2016).
[91] U. Bhattacharya, S. Bandyopadhyay, and A. Dutta, Mixed state dynamical quantum phase transitions, Phys. Rev. B **96**, 180303(R) (2017).
[92] N. Fläschner, D. Vogel, M. Tarnowski, B. S. Rem, D.-S. Lühmann, M. Heyl, J. C. Budich, L. Mathey, K. Sengstock, and C. Weitenberg, Observation of dynamical vortices after quenches in a system with topology, Nature Phys. **14**, 265 (2018).
[93] P. Jurcevic, H. Shen, P. Hauke, C. Maier, T. Brydges, C. Hempel, B. P. Lanyon, M. Heyl and, R. Blatt, and C. F. Roos, Direct observation of dynamical quantum phase transitions in an interacting many-body system, Phys. Rev. Lett. **119**, 080501 (2017).
[94] E. A. Martinez, C. A. Muschik, P. Schindler, D. Nigg, A. Erhard, M. Heyl, P. Hauke, M. Dalmonte, T. Monz, P. Zoller *et al.*, Real-time dynamics of lattice gauge theories with a few-qubit quantum computer, Nature (London) **534**, 516 (2016).
[95] X.-Y. Guo, C. Yang, Y. Zeng, Y. Peng, H.-K. Li, H. Deng, Y.-R. Jin, S. Chen, D. Zheng, and H. Fan, Observation of a dynamical quantum phase transition by a superconducting qubit simulation, Phys. Rev. Appl. **11**, 044080 (2019).
[96] K. Wang, X. Qiu, L. Xiao, X. Zhan, Z. Bian, W. Yi, and P. Xue, Simulating dynamic quantum phase transitions in photonic quantum walks, Phys. Rev. Lett. **122**, 020501 (2019).
[97] X. Nie, B.-B. Wei, X. Chen, Z. Zhang, X. Zhao, C. Qiu, Y. Tian, Y. Ji, T. Xin, D. Lu, and J. Li, Experimental observation of equilibrium and dynamical quantum phase transitions via out-of-time-ordered correlators, Phys. Rev. Lett. **124**, 250601 (2020).
[98] F. J. González, A. Norambuena, and R. Coto, Dynamical quantum phase transition in diamond: Applications in quantum metrology, Phys. Rev. B **106**, 014313 (2022).
[99] H. Pichler, J. Schachenmayer, J. Simon, P. Zoller, and A. J. Daley, Noise- and disorder-resilient optical lattices, Phys. Rev. A **86**, 051605(R) (2012).
[100] P. Zoller, G. Alber, and R. Salvador, ac stark splitting in intense stochastic driving fields with gaussian statistics and non-lorentzian line shape, Phys. Rev. A **24**, 398 (1981).
[101] X. Chen, A. Ruschhaupt, S. Schmidt, A. del Campo, D. Guéry-Odelin, and J. G. Muga, Fast optimal frictionless atom cooling in harmonic traps: Shortcut to adiabaticity, Phys. Rev. Lett. **104**, 063002 (2010).
[102] P. Doria, T. Calarco, and S. Montangero, Optimal control technique for many-body quantum dynamics, Phys. Rev. Lett. **106**, 190501 (2011).
[103] J. Marino and A. Silva, Relaxation, prethermalization, and diffusion in a noisy quantum Ising chain, Phys. Rev. B **86**, 060408(R) (2012).
[104] J. Marino and A. Silva, Nonequilibrium dynamics of a noisy quantum Ising chain: Statistics of work and prethermalization after a sudden quench of the transverse field, Phys. Rev. B **89**, 024303 (2014).
[105] A. Dutta, A. Rahmani, and A. del Campo, Anti-kibble-zurek behavior in crossing the quantum critical point of a thermally isolated system driven by a noisy control field, Phys. Rev. Lett. **117**, 080402 (2016).
[106] Y. Bando, Y. Susa, H. Oshiyama, N. Shibata, M. Ohzeki, F. J. Gómez-Ruiz, D. A. Lidar, S. Suzuki, A. del Campo, and H. Nishimori, Probing the universality of topological defect formation in a quantum annealer: Kibble-zurek mechanism and beyond, Phys. Rev. Res. **2**, 033369 (2020).
[107] A. Chenu, M. Beau, J. Cao, and A. del Campo, Quantum simulation of generic many-body open system dynamics using classical noise, Phys. Rev. Lett. **118**, 140403 (2017).
[108] A. Dutta and A. Dutta, Probing the role of long-range interactions in the dynamics of a long-range Kitaev chain, Phys. Rev. B **96**, 125113 (2017).
[109] P. Uhrich, N. Defenu, R. Jafari, and J. C. Halimeh, Out-of-equilibrium phase diagram of long-range superconductors, Phys. Rev. B **101**, 245148 (2020).
[110] J. C. Xavier and J. A. Hoyos, Effect of long-range hopping on dynamic quantum phase transitions of an exactly solvable free-fermion model: Nonanalyticities at almost all times, Phys. Rev. B **108**, 214303 (2023).
[111] M. Syed, T. Enss, and N. Defenu, Dynamical quantum phase transition in a bosonic system with long-range interactions, Phys. Rev. B **103**, 064306 (2021).
[112] B. Žunkovič, M. Heyl, M. Knap, and A. Silva, Dynamical quantum phase transitions in spin chains with long-range interactions: Merging different concepts of nonequilibrium criticality, Phys. Rev. Lett. **120**, 130601 (2018).
[113] U. Mishra, R. Jafari, and A. Akbari, Disordered Kitaev chain with long-range pairing: Loschmidt echo revivals and dynamical phase transitions, J. Phys. A: Math. Theor. **53**, 375301 (2020).
[114] T. Masłowski and N. Sedlmayr, The dynamical bulk boundary correspondence and dynamical quantum phase transitions in the Benalcazar–Bernevig–Hughes model, J. Phys. Condens. Matter, **36**, 335401 (2024).
[115] R. Jafari, A. Langari, S. Eggert, and H. Johannesson, Dynamical quantum phase transitions following a noisy quench, Phys. Rev. B **109**, L180303 (2024).
[116] U. Divakaran, S. Sharma, and A. Dutta, Tuning the presence of dynamical phase transitions in a generalized XY spin chain, Phys. Rev. E **93**, 052133 (2016).
[117] S. Sharma, U. Divakaran, A. Polkovnikov, and A. Dutta, Slow quenches in a quantum Ising chain: Dynamical phase transitions and topology, Phys. Rev. B **93**, 144306 (2016).

[118] B. Dóra, F. Pollmann, J. Fortágh, and G. Zaránd, Loschmidt echo and the many-body orthogonality catastrophe in a qubit-coupled luttinger liquid, Phys. Rev. Lett. **111**, 046402 (2013).

[119] S. Bhattacharjee and A. Dutta, Dynamical quantum phase transitions in extended transverse Ising models, Phys. Rev. B **97**, 134306 (2018).

[120] S. Sharma, A. Russomanno, G. E. Santoro, and A. Dutta, Loschmidt echo and dynamical fidelity in periodically driven quantum systems, Europhys. Lett. **106**, 67003 (2014).

[121] A. Y. Kitaev, Unpaired majorana fermions in quantum wires, Phys. Usp. **44**, 131 (2001).

[122] S. Ryu and Y. Hatsugai, Topological origin of zero-energy edge states in particle-hole symmetric systems, Phys. Rev. Lett. **89**, 077002 (2002).

[123] A. Alecce and L. Dell'Anna, Extended Kitaev chain with longer-range hopping and pairing, Phys. Rev. B **95**, 195160 (2017).

[124] A. Solfanelli, S. Ruffo, S. Succi, and N. Defenu, Logarithmic, fractal and volume-law entanglement in a Kitaev chain with long-range hopping and pairing, J. High Energy Phys. 05 (2023) 066.

[125] S. Nadj-Perge, I. K. Drozdov, J. Li, H. Chen, S. Jeon, J. Seo, A. H. MacDonald, B. A. Bernevig, and A. Yazdani, Observation of majorana fermions in ferromagnetic atomic chains on a superconductor, Science **346**, 602 (2014).

[126] M. Ruby, B. W. Heinrich, Y. Peng, F. von Oppen, and K. J. Franke, Exploring a proximity-coupled Co chain on Pb (110) as a possible majorana platform, Nano Lett. **17**, 4473 (2017).

[127] G. Szegö, A. Erdélyi, W. Magnus, F. Oberhettinger and F. G. Tricomi, Higher transcendental functions, Bull. Am. Math. Soc. **60**, 405 (1954).

[128] M. Abramowitz, I. A. Stegun, and R. H. Romer, Handbook of mathematical functions with formulas, graphs, and mathematical tables, Am. J. Phys. **56**, 958 (1988).

[129] J. Łuczka, Quantum open systems in a two-state stochastic reservoir, Czech. J. Phys. **41**, 289 (1991).

[130] A. A. Budini, Non-markovian gaussian dissipative stochastic wave vector, Phys. Rev. A **63**, 012106 (2000).

[131] J. I. Costa-Filho, R. B. B. Lima, R. R. Paiva, P. M. Soares, W. A. M. Morgado, R. L. Franco, and D. O. Soares-Pinto, Enabling quantum non-markovian dynamics by injection of classical colored noise, Phys. Rev. A **95**, 052126 (2017).

[132] A. Kiely, Exact classical noise master equations: Applications and connections, Europhys. Lett. **134**, 10001 (2021).

[133] N. V. Vitanov and B. M. Garraway, Landau-Zener model: Effects of finite coupling duration, Phys. Rev. A **53**, 4288 (1996).

[134] N. V. Vitanov, Transition times in the Landau-Zener model, Phys. Rev. A **59**, 988 (1999).